Stochastic Active Observers: Active State Analysis - Theory and A Robotic Force Control Application

Rui Cortesão,[†] Ralf Koeppe,[‡] Urbano Nunes,[†] and Gerd Hirzinger [‡]

[†]University of Coimbra
Institute of Systems and Robotics - ISR
3030 Coimbra, Portugal
Fax: +351 239 406672
Email: cortesao@isr.uc.pt

[‡]German Aerospace Center - DLR
Institute of Robotics and Mechatronics
82230 Wessling, Germany
Fax: +49 8153 281134
E-mail: Ralf.Koeppe@dlr.de

Abstract

The paper introduces the Active Observer (AOB) concept in the framework of stochastic theory. The overall AOB control structure is discussed on a conceptual level, enabling its implementation in any control system, coming or not from the robotics field. The AOB concept was initially discussed in [3]. The paper extends the analysis of the AOB with respect to the active state. Simulation results comparing the force tracking capabilities of the AOB and the Classical Kalman Filter (CKF) are presented, showing the importance of the active state.

1 Introduction

In robotic control systems, unknown disturbances, higher order dynamics, nonlinearities and noise are always present. Particularly, if the robot is doing compliant motion tasks that require contact with unknown environments, "rigid" model-based approaches are seldom efficient, and the robustness of the task execution can be seriously deteriorated if unmodeled disturbances are not handled in a proper way. Recently, several methods have been presented to deal with disturbances. In [8], an extended deterministic observer is constructed to estimate the motion parameters of a moving object in a force control task. In [1], model uncertainties, nonlinearities, and external disturbances are merged to one term, and then compensated with a non-linear disturbance observer, based on the variable structure system (VSS) theory. Several drawbacks of previous methods, like the approximate differentiator and the H_∞ type formulations are also pointed out in [1]. In [5], a neural network approach is used as a compensator to cancel out all the uncertainties occurred in force control, such as robot model mismatches, unknown environment stiffness and location. A manipulator control method using a disturbance observer with no inverse dynamics is addressed in [7].

The proposed AOB structure uses a self-adjusting discrete probabilistic approach to estimate disturbances. The method has a systematic formulation, is mathematically elegant, and uses the Kalman theory with new interpretations to optimise its performance function of system and measurement noises.

2 AOB Concept

Given a linear system represented in state-space form by

$$x_n = \Phi x_{n-1} + \Gamma u_{n-1}, \tag{1}$$

any linear controller can be achieved with state feedback (optimal control, adaptive control, deadbeat control, "pure" pole placement control, etc.). In practice, the main problem of this approach is that the model of the system in Equation (1) does not represent exactly the real system. In fact, higher order dynamics, noise, unknown disturbances, etc., are not addressed in the plant model. Therefore, it is necessary to develop a control structure that can deal with unmodeled terms, so that the overall system has the desired closed-loop dynamics. The AOB state-space control design satisfies these requirements. **The main goal of the AOB is to impose to the overall system a desired closed-loop behaviour, regardless the imperfect model of the plant.** An active state p_k (extra-state) is introduced to compensate unmodeled terms, providing a feedforward compensation action. A stochastic equation is used to describe the active state,

$$p_k - p_{k-1} = w_k. \tag{2}$$

Equation (2) only says that the discrete derivative of p_k is randomly distributed. It gives no explicit information about the p_k characteristics. Hence, arbitrary disturbances can be estimated (model-free equation). In fact, the general form of Equation (2) is

$$p_k = \sum_{j=1}^{R}(-1)^{j+1}\frac{R!}{j!(R-j)!}p_{k-j} +^R w_k, \tag{3}$$

where ${}^R w_k$ describes the R^{st} derivative of the process to estimate [2]. From Equation (2), the disturbance p_{k-1} can go

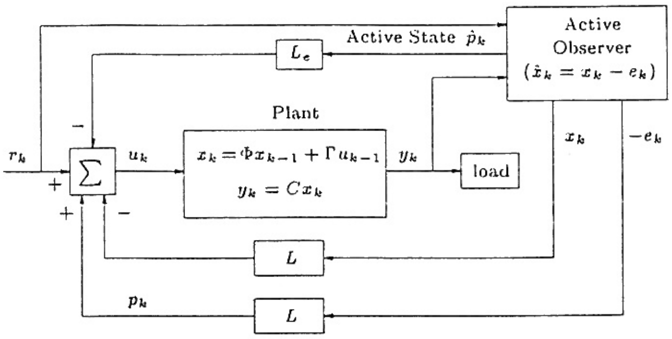

Figure 1: Active Observer. Emphasis in the active state $\hat{p}_k$ that compensates the error e_k referred to the system input. $L_e = 1$, and L are the state feedback gains.

to any value at time k with a certain probability of occurrence. It is based on the stochastic properties of w_k that this probability is computed. **In the AOB context, only the variance of $\mathbf{w_k}$ is needed to estimate the active state $\mathbf{p_k}$.**

2.1 AOB Structure

Figure 1 shows a generic control system with the AOB in the loop. **The error $\mathbf{e_k}$ can be seen as an additional system input that needs to be compensated.** An extra state variable is necessary to perform the compensation of e_k. However, the Classical Observer structure cannot "see" e_k. The observer receives the input to the system u_k given by

$$u_k = r_k - Lx_k + p_k, \tag{4}$$

where the disturbance referred to the system input is $p_k = Le_k$. Hence, the Classical Observer cannot distinguish p_k from r_k. To overcome this difficulty, the observer ought to know the reference r_k instead of u_k. The real system should have the behaviour

$$x_k = \Phi\, x_{k-1} + \Gamma(r_{k-1} - Lx_{k-1}). \tag{5}$$

Defining the closed-loop matrix $\Phi_c = \Phi - \Gamma L$, Equation (5) is written as

$$x_k = \Phi_c\, x_{k-1} + \Gamma r_{k-1}. \tag{6}$$

Thus, the observer equation should only reflect these changes. This approach can only be generalised when the closed-loop system is observable. There are some cases, where the state feedback is used to eliminate the influence of an undesired state in all the others, originating a non-observable closed-loop system. This is precisely what happens with Active Observers. The active state $\hat{p}_k$ estimates the error e_k referred to the system input, permitting the overall system to have the ideal behaviour. The closed-loop system is clearly non-observable, because the influence of this state is canceled at the system input. To get off this difficulty, the observer design considers that the system is in open loop. Then, in the state estimate $\hat{x}_k$, Equation (6) is used. More details of the AOB algorithm are given in [3], [4].

2.2 The AOB Algorithm

The AOB algorithm is described in this section. Detailed analysis can be seen in [4] and [3].

The *a priori* state estimate $\hat{x}_k^-$ is

$$\hat{x}_k^- = \Phi_{ac}\, \hat{x}_{k-1} + \Gamma r_{k-1}. \tag{7}$$

Giving the measure y_k, the *a priori* estimation error e_k^- is

$$e_k^- = y_k - C\hat{x}_k^-. \tag{8}$$

Finally, the corrected estimation,

$$\hat{x}_k = \hat{x}_k^- + K_k e_k^-, \tag{9}$$

where K_k is the Kalman gain,

$$K_k = P_{1k}\, C^T \left[C\, P_{1k}\, C^T + R_k\right]^{-1}, \tag{10}$$

and

$$P_{1k} = \Phi_a\, P_{k-1}\, \Phi_a^T + Q_k, \tag{11}$$

with

$$P_k = P_{1k} - K_k\, C\, P_{1k}. \tag{12}$$

Q_k is the system noise matrix, and its interpretation is discussed in Sections 3.2 and 3.3. R_k is the measurement noise matrix and is function of the measurement noise η_k, $R_k = E\{\eta_k \eta_k^T\}$. The open loop and the closed-loop system matrices are given by Φ_a and $\Phi_{ac} = (\Phi_a - \Gamma L)$ respectively, and include already the active state, i.e.

$$\Phi_a = \begin{bmatrix} \Phi & \Gamma_1 & \Gamma_0 & \cdots & 0 & 0 \\ 0 & 0 & 1 & \cdots & 0 & 0 \\ \vdots & \vdots & \vdots & \ddots & \vdots & \vdots \\ 0 & 0 & 0 & \cdots & 1 & 0 \\ 0 & 0 & 0 & \cdots & 0 & 1 \\ 0 & 0 & 0 & \cdots & 0 & 1 \end{bmatrix}, \tag{13}$$

$$\Phi_{ac} = \begin{bmatrix} \Phi & \Gamma_1 & \Gamma_0 & \cdots & 0 & 0 \\ 0 & 0 & 1 & \cdots & 0 & 0 \\ \vdots & \vdots & \vdots & \ddots & \vdots & \vdots \\ 0 & 0 & 0 & \cdots & 1 & 0 \\ -L_1 & -L_2 & -L_3 & \cdots & -L_{n-1} & 0 \\ 0 & 0 & 0 & \cdots & 0 & 1 \end{bmatrix}, \tag{14}$$

$$\Gamma = \begin{bmatrix} 0 & 0 & \cdots & 0 & 1 & 0 \end{bmatrix}^T. \tag{15}$$

The non-augmented open-loop Φ_{ar} and command Γ_r matrices are

$$\Phi_{ar} = \begin{bmatrix} \Phi & \Gamma_1 & \Gamma_0 & \cdots & 0 \\ 0 & 0 & 1 & \cdots & 0 \\ \vdots & \vdots & \vdots & \ddots & \vdots \\ 0 & 0 & 0 & \cdots & 1 \\ 0 & 0 & 0 & \cdots & 0 \end{bmatrix}, \tag{16}$$

and

$$\Gamma_r = \begin{bmatrix} 0 & 0 & \cdots & 0 & 1 \end{bmatrix}^T. \tag{17}$$

The L components are obtained by Ackermann's formula for the non-augmented system, given a desired closed-loop behaviour. The state x_k is

$$x_k = \left[\begin{array}{cccccc} x_k^{'} & u_{k-d} & \cdots & u_{k-2} & u_{k-1} & p_k \end{array}\right]^T, \quad (18)$$

where $x_k^{'}$ is the state of the system considering no dead-time. u_{k-m} are the delayed command efforts, and p_k is the active state.

The CKF can be obtained from the AOB with small changes. Only the active state is eliminated from the estimation, i.e. $\hat{p}_k = 0$, and its corresponding value in the Q_k matrix is set to zero. Re-designing the Q_k matrix is needed in some cases. The explanation is beyond the scope of this paper.

3 Active State: A Probabilistic Approach

To cope with parameter variations, unmodeled nonlinear terms and unpredicted disturbances, lumped in the p_k variable, an active state $\hat{p}_k$ is created. Several possibilities can be considered. For a Deterministic Active Observer, a model for the error dynamics of p_k is needed. The simplest case is for a constant error, giving a state equation of the form $p_k = p_{k-1}$. For a time varying error, the state equation changes. Clearly there are obvious limitations in the deterministic approach. It becomes natural to use stochastic concepts to quantify disturbances, enabling a wide class of signals to be described with the same equation. A stochastic model was developed to deal with unknown disturbances [2]. Looking to Equation (2), the stochastic process $\{w_k\}$ can be seen as the first order active state evolution. Let's define w_k^o as one realisation of the process at time k. All the random variables w_k have a Gaussian distribution with zero mean and variance $\sigma_{w_k}^2$. w_k represents the evolution (change) in p_k from time $k-1$ to time k. Defining the estimation strategy as:

The probability of the $\mathbf{p_k}$ evolution (in module) be greater than its previous evolution (in module), should be equal to α_k,

the variance of w_k is computed in a straightforward way. The value α_k can change on-line as a function of the task state. Qualitatively, if α_k is big, it means that p_k is able to follow high frequency signals. On the other hand, if α_k is low, only low frequency signals are estimated. In formal terms,

$$w_k \sim N(0, \sigma_{w_k}^2). \quad (19)$$

The strategy is

$$P(|w_k| > |w_{k-1}^o|) = \alpha_k, \quad \text{with} \quad 0 < \alpha_k < 1. \quad (20)$$

Defining a new random variable

$$\chi_k \sim N(0,1), \quad (21)$$

Equation (20) is written as

$$P(|\chi_k| > \left|\frac{w_{k-1}^o}{\sigma_{w_k}}\right|) = \alpha_k, \quad (22)$$

which has a well known solution. Defining the function G as

$$G(x) = \int_x^{\infty} \frac{1}{\sqrt{2\pi}} e^{-\frac{\lambda^2}{2}} d\lambda, \quad (23)$$

the solution of Equation (22) is given by

$$\sigma_{w_k} = \frac{|w_{k-1}^o|}{G^{-1}(\alpha_k/2)}, \quad (24)$$

where G^{-1} is the inverse function of G. The function $G(x)$ cannot be obtained explicitly, but many software libraries provide a related function, the error function erf, defined as

$$\mathrm{erf}(x) = \frac{2}{\sqrt{\pi}} \int_0^x e^{-t^2} dt. \quad (25)$$

Hence,

$$G(x) = \frac{1 - \mathrm{erf}(x/\sqrt{2})}{2}, \quad (26)$$

and Equation (24) can be written as

$$\sigma_{w_k} = \frac{|w_{k-1}^o|}{\sqrt{2}\,\mathrm{erf}^{-1}(1-\alpha_k)}. \quad (27)$$

The variance of w_k, $\sigma_{w_k}^2$, is computed from Equation (27), which is in the Kalman notation the Q_k value for the active state. Thus, the p_k estimation is done in the framework of probabilistic estimation. If w_k is a narrow-band process, good results are achieved for a constant α_k. However, for wide-band processes, a dynamic assignment of α_k is needed. When $w_k^0 \to 0$, a minimum σ_{w_k} should be imposed, so that the p_k estimation is able to follow abrupt changes, with an acceptable time-lag. The price payed for this, is that around low frequency values, the noise sensitivity is increased.

3.1 Computation of α_k for the Desired Minimum σ_{w_k}

The function e^{-t^2} can be written in Taylor Series around zero, giving

$$e^{-t^2} = 1 - t^2 + \frac{t^4}{2!} - \frac{t^6}{3!} + \cdots, \quad (28)$$

and,

$$\int_0^x e^{-t^2} dt = x - \frac{x^3}{3} + \frac{x^5}{5 \cdot 2!} - \frac{x^7}{7 \cdot 3!} + \cdots. \quad (29)$$

From Equations (25) and (29),

$$\lim_{x \to 0} \mathrm{erf}(x) \approx \frac{2x}{\sqrt{\pi}}. \quad (30)$$

Using Equation (30), straightforward analysis gives,

$$\lim_{x \to 0} \frac{\mathrm{erf}^{-1}(bx)}{x} = b\frac{\sqrt{\pi}}{2}. \quad (31)$$

Looking to Equations (27) and (31), a minimum value of σ_{w_k}, $\sigma_{w_k}^*$, is achieved for very weak p_k evolutions, $|w_{k-1}^0| \ll 1$, only if

$$\alpha_k = 1 - \frac{\sqrt{2/\pi}}{\sigma_{w_k}^*} |w_{k-1}^0|. \quad (32)$$

3.2 Qualitative Meaning of the Q_k Matrix for the Active State p_k

The Q_k matrix is written as

$$Q_k = \sigma^2_{w_k}, \tag{33}$$

and its interpretation is qualitatively defined by the estimation strategy, i.e. the value of α_k at each time step. It is the responsibility of the control designer to input proper values of α_k, in order to have good performance in the p_k estimation. For a given Q_k value, Equation (27) says that the strategy is

$$\alpha_k = 1 - \mathrm{erf}(\frac{|w^0_{k-1}|}{\sqrt{2Q_k}}). \tag{34}$$

It can be inferred from Equation (34), that even for a constant Q_k value, the strategy changes at each time step, lying in the framework of stochastic adaptive estimation. To keep always the same strategy, it is necessary that

$$Q_k = \frac{|w^0_{k-1}|^2}{c^2}, \tag{35}$$

where c is a constant, giving then

$$\alpha_k = 1 - \mathrm{erf}(\frac{c}{\sqrt{2}}). \tag{36}$$

Figure 2 presents a schematic overview of the estimation strategy for the active state. The variance $\sigma^2_{w_k}$ is computed at each time step, function of α_k and $|w^o_{k-1}|$. Using this information, the p_k estimate is computed. The stochastic process $\{w_n\}$ is represented in Figure 2.a. At each time step, there is a random variable w_k, with a Gaussian distribution of zero mean and variance $\sigma^2_{w_k}$. One realization of the process $\{w_n\}$ is shown in Figure 2.b, obtained from the p_n estimation, displayed in Figure 2.c. Of course, other strategies can be defined, giving different meanings for the Q_k values. This is one of the rich characteristics of stochastic analysis. The Q_k values can be interpreted according to some context. The designer should define the strategy in an intuitive way for a given problem in order to input proper numerical values. Another strategy is defined for the other state variables in Section 3.3, with some interesting "symmetric" properties.

3.3 Qualitative Meaning of the Q_k Matrix for the State x_k

A generic system represented in state-space form is given by

$$x_k = \Phi\, x_{k-1} + \Gamma u_{k-1} + \xi_k, \tag{37}$$

where u_{k-1} is the command input, and ξ_k is a random vector (sometimes called system noise vector) associated with the state x_k. Equation (37) says that x_k has a deterministic term function of x_0 and u_{k-1}, and a random term function of the statistical properties of ξ_k. This section analyses only the role of the random term in x_k. Then, since the system is linear, the superposition theorem can be applied to get the full solution of Equation (37). For the random term,

$$x_k = \Phi\, x_{k-1} + \xi_k. \tag{38}$$

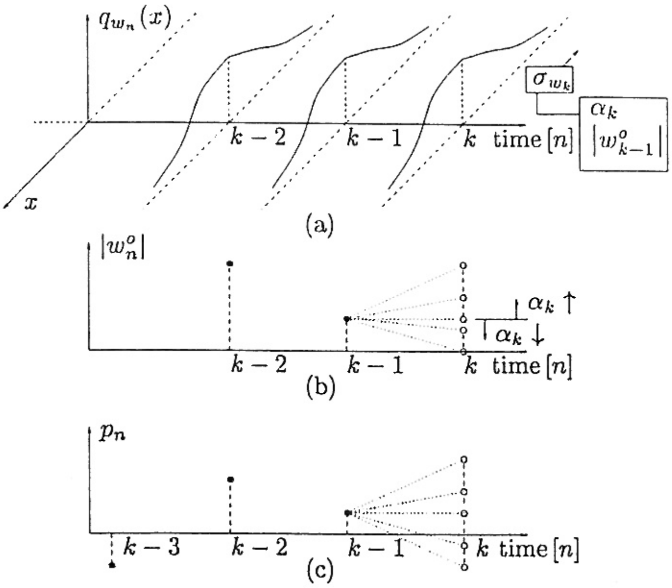

Figure 2: Representation of the stochastic adaptive estimation for the active state p_n. (a) **The stochastic process $\{w_n\}$.** $q_{w_n}(x)$ represents the probability density function (pdf) of w_n. At each time step, the variance of w_n, i.e. the Q_n value, is computed function of the present strategy α_n, and of the previous active state evolution $|w^o_{n-1}|$. (b) **One realisation of the process $\{w_n\}$.** The value $|w^o_{k-2}| = |p_{k-3} - p_{k-2}|$, and $|w^o_{k-1}| = |p_{k-2} - p_{k-1}|$. The active state evolution at time k is function of α_k, i.e. a bigger α_k allows bigger p_k evolutions. (c) **Time plot of the active state p_n.**

If the process $\{\xi_k\}$ is a zero mean white Gaussian sequence independent of the initial condition x_0, then given x_{k-1}, x_k depends only on ξ_k, which is independent of the previous states. Hence, the process $\{x_k\}$ is a Gauss-Markov process (GMP). The probability density functions of x_k can be calculated according to the GMP properties. The inverse function of Equation (38) is

$$\xi_k = x_k - \Phi\, x_{k-1}. \tag{39}$$

The Jacobian determinant is one, and assuming that,

$$\begin{array}{rcl} x_k & = & [x_{1_k} \quad x_{2_k} \quad \cdots, \quad x_{N_k}]^T, \text{ and} \\ \xi_k & = & [\xi_{1_k} \quad \xi_{2_k} \quad \cdots, \quad \xi_{N_k}]^T, \end{array} \tag{40}$$

the conditional probability density function is,

$$\begin{array}{l} p_{x_{1_k}, x_{2_k}, \cdots, x_{N_k}|x_{k-1}}(x_{1_k}, x_{2_k}, \cdots, x_{N_k}|x_{k-1}) \\ = p_{\xi_{1_k}, \xi_{2_k}, \cdots, \xi_{N_k}|x_{k-1}}(x_{1_k} - \Phi_1 x_{k-1}, \\ x_{2_k} - \Phi_2 x_{k-1}, \cdots, x_{N_k} - \Phi_N x_{k-1}). \end{array} \tag{41}$$

where Φ_i is the i^{th} line of matrix Φ. In other words,

$$\begin{array}{l} p_{x_{1_k}|x_{k-1}}(x_{1_k}|x_{k-1}) \\ = \int \cdots \int p_{\xi_{1_k}, \xi_{2_k}, \cdots, \xi_{N_k}|x_{k-1}}(x_{1_k} \\ -\Phi_1 x_{k-1}, x_{2_k} - \Phi_2 x_{k-1}, \\ \cdots, x_{N_k} - \Phi_N x_{N_{k-1}}) \cdot dx_{N_k} dx_{N-1_k} \cdots, dx_{2_k}. \end{array} \tag{42}$$

In most of real applications, the ξ_{i_k} $(i = 1, \cdots, N)$ variables are not correlated (they are orthogonal). Equation (42) becomes,

$$p_{x_{i_k}|x_{k-1}}(x_{i_k}|x_{k-1}) = p_{\xi_{i_k}}(x_{i_k} - \Phi_i x_{k-1}), \text{ with } i = 1, \cdots, N. \tag{43}$$

For a Gaussian distribution of ξ_{i_k}, Equation (43) is

$$p_{x_{i_k}|x_{k-1}}(x_{i_k}|x_{k-1}) = \frac{1}{\sqrt{2\pi Q_{i_k}}} e^{-\frac{(x_{i_k} - \Phi_i x_{k-1})^2}{2Q_{i_k}}}. \tag{44}$$

The expected value for x_{i_k} given x_{k-1} is $\Phi_i x_{k-1}$, i.e. the "noise-free" situation. The variance around this value is given by Q_{i_k}. If $Q_{i_k} \to 0$, Equation (44) becomes a Dirac delta function centered around $x_{i_k} = \Phi_i x_{k-1}$, which is the deterministic case. The bigger Q_k is, the bigger the uncertainty around the expected value is. Defining now the strategy as: **Given $\mathbf{x}_{k-1}$, the probability of the deviation (in module) of $\mathbf{x}_{i_k}$ around the expected value $\mu_{\mathbf{x}_{i_k}} = \Phi_i \mathbf{x}_{k-1}$ be greater than γ_{i_k} should be equal to β_{i_k}**, i.e.

$$p_{x_{i_k}|x_{k-1}}\left(|x_{i_k} - \mu_{x_{i_k}}| > \gamma_{i_k}\right) = \beta_{i_k}, \tag{45}$$

the value $\sigma_{x_{i_k}} = \sqrt{Q_{i_k}}$ can be calculated in a straightforward way, and is given by,

$$\sigma_{x_{i_k}} = \frac{\gamma_{i_k}}{\sqrt{2}\ \mathrm{erf}^{-1}(1 - \beta_{i_k})}. \tag{46}$$

Equation (46) should be compared with Equation (27). There are multiple solutions for the same strategy β_{i_k}. An interesting one is obtained when $\gamma_{i_k} = \sigma_{x_{i_k}}$, giving then

$$\beta_{i_k} = 1 - \mathrm{erf}\left(\sqrt{2}/2\right), \tag{47}$$

i.e. $\beta_{i_k} = 0.3173$. Therefore, the probability of the signal deviation around the expected value be greater than $\sigma_{x_{i_k}}$ is about thirty per cent. This procedure is also valid for the active state ($\Phi = 1$), giving another interpretation for the Q_k value. All these interpretations provide useful guidelines to design the Q_k matrix for a given application. However, it should be noted that for the Kalman AOB, the Q_k matrix by itself does not describe the system. The measurement noise matrix R_k has a key role in the estimation process. The balance between model uncertainties given by Q_k and measure uncertainties given by R_k defines the steady-state Kalman gains, that influence the convergence rate of the estimates.

4 AOB vs. CKF: Force Tracking Capabilities

An application of the AOB/CKF in a robotic force tracking task is analysed in this section. In a multi-dimensional compliant motion task, there are couplings between motion and force. Figure 3 illustrates an example where a movement in y direction disturbs the force controller in x direction, since the surface geometry in x changes with time. The velocity disturbance $\dot{x}_{\text{dist}}$ is given by

$$\dot{x}_{\text{dist}} = \frac{x_1 - x_0}{y_1 - y_0} v_y, \tag{48}$$

where x_0, x_1, y_0, y_1 are geometric coordinates, and v_y is the velocity in y. x_{dist} enters in the system with negative sign (Figure 4). If x_{dist} has a negative derivative, the velocity disturbance referred to the system input is positive, creating a ΔF in the force response, if no compensation action is performed. This ΔF creates a barrier to the maximum v_y. In many tasks, velocity scaling is necessary, to prevent high ΔF. In the simulations, each degree of freedom of the the position controlled robot represented in Figure 4 has the transfer function

$$G_r(s) = \frac{1}{1 + T_p s} e^{-T_D s}, \tag{49}$$

that is equal to one in steady state. K_s is the system stiffness. In this way, for a disturbance x_{dist}, the feedforward velocity should be equal to $\dot{x}_{\text{dist}}$. Several possibilities can be applied to compensate geometric changes by adding position or velocity feedforward information to the system. The feedforward action can be generated [6]: 1) from *a priori* information, 2) by external geometric sensing, 3) from position and force measurements, and 4) from the output of a skill map, trained from human demonstration data. However, if the AOB is used in the controller, the active state estimates the position disturbance, providing a proper compensation action. On the other hand, if the controller has an observer without active state, like the CKF, the force error is function of the Kalman gains. Simulation tools showed that the force error is

$$\Delta F_{ss} \approx 0.6839\, K_s \dot{x}_e, \tag{50}$$

where K_s is the system stiffness and $\dot{x}_e$ is the feedforward compensation error of the velocity. Figure 5 shows the performance of the force controller with AOB and CKF when geometric changes occur during the task. The surface changes at 8 [s] with a negative slop. The active state performs the feedforward compensation action, that converges to the surface derivative (Figures 5.b and 5.d). In this simulation the system stiffness $K_s = 3$. For the CKF there is no external feedforward action, therefore, the error $\dot{x}_e$ is equal to $-\dot{x}_{\text{dist}}$. Using Equation (50), $\Delta F_{ss} \approx 4.1034$. When the AOB is used, the steady state error disappears, and the transient ΔF is reduced (Figures 5.a and 5.c). The strategy for the active state is an adaptive one: $Q_k = 10^{-5}$, and α_k is computed from Equation (34), that is function of the on-line data. For the other states, $\gamma_{ik} = 10^{-12}$, and β_{ik} is given by Equation (47). In our robotic application, the AOB algorithm described in Section 2.2 was applied with the following values: $d = 5$, $k_1 = K_s/T_p$, $p_1 = 1/T_p$, the feedback gains L were obtained for a critically damped system with a time constant $\tau = 10/T_p$. Finally,

$$\Phi = \phi(h) = \begin{bmatrix} 1 & \frac{1 - e^{-p_1 h}}{p_1} \\ 0 & e^{-p_1 h} \end{bmatrix}, \tag{51}$$

$$\Gamma_0 = \begin{bmatrix} 0 \\ 0 \end{bmatrix}, \quad \text{and} \quad \Gamma_1 = \frac{k_1}{p_1} \begin{bmatrix} h + \frac{e^{-p_1 h} - 1}{p_1} \\ 1 - e^{-p_1 h} \end{bmatrix}. \tag{52}$$

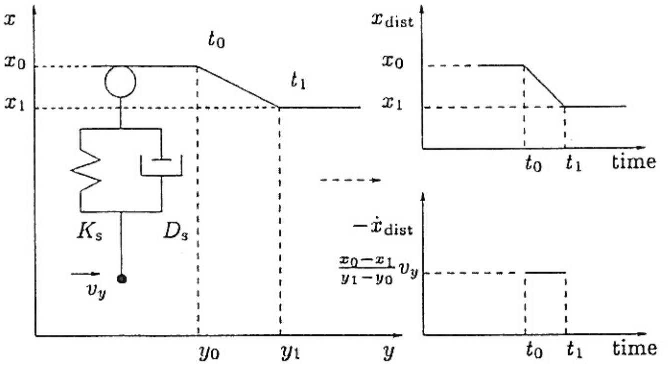

Figure 3: Coupling between constrained and unconstrained directions. K_s and D_s are the stiffness and damping in the x direction, respectively. The damping is not considered in the force control simulations.

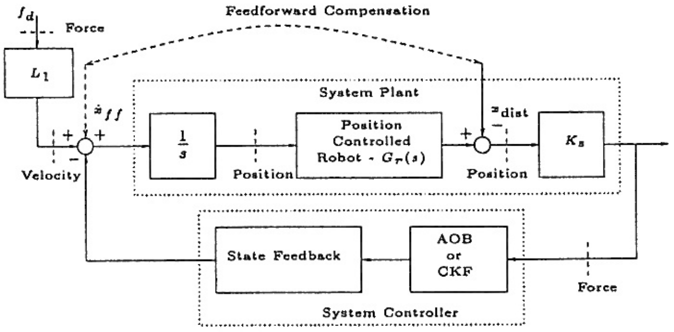

Figure 4: Feedforward compensation due to surface changes during the task execution. If the AOB is used in the control loop, the feedfoward term is automatically generated by the active state. If output feedback, or the CKF is used, the feedforward velocity should be given by an external source.

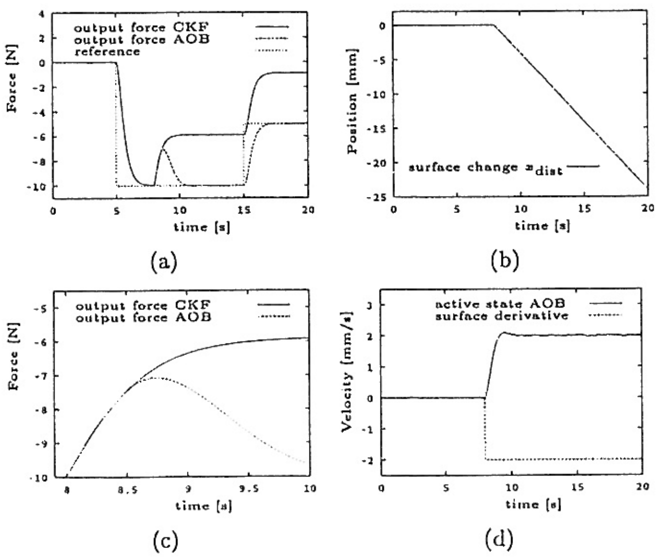

Figure 5: Force tracking capabilities when the contact surface changes with time. (a) AOB vs. CKF, (b) The contact surface, (c) Detailed view of (a), and (d) Active state vs. contact surface derivative.

5 Conclusions

The paper introduces the AOB concept, and analyses the active state in the framework of stochastic theory. The AOB algorithm is described. The CKF can be obtained from the AOB with minimal changes. Several strategies can be followed, to input adequate values in the AOB design. This procedure is also extended to the other state variables of the system. The comparison between AOB and CKF is done in a force control application.

Acknowledgements

This work is partially supported by FCT (Portuguese Science and Technology Foundation) project number PCTI/1999/SRI/33594, and by the FCT Ph.D. grant SFRH/BD/2754/2000.

References

[1] X. Chen, S. Komada, and T. Fukuda. Design of a nonlinear disturbance observer. *IEEE Trans. on Industrial Electronics*, 47(2):429–435, April 2000.

[2] R. Cortesão and R. Koeppe. Sensor fusion for human-robot skill transfer systems. *RSJ Int. J. on Advanced Robotics. Special Issue on Selected Papers from IROS'99*, 14(6):537–550, 2000.

[3] R. Cortesão, R. Koeppe, U. Nunes, and G. Hirzinger. Explicit force control for manipulators with active observers. In *Proc. of the 2000 IEEE Int. Conf. on Intelligent Robots and Systems, (IROS'2000)*, volume 2, pages 1075–1080, Japan, 2000.

[4] R. Cortesão, R. Koeppe, U. Nunes, and G. Hirzinger. Force control with a kalman active observer applied in a robotic skill transfer system. *Int. J. on Machine Intelligence and Robotic Control (MIROC). Special Issue on Force Control of Advanced Robotic Systems*, 2(2):59–68, June 2000.

[5] S. Jung and T. Hsia. Robust neural force control scheme under uncertainties in robot dynamics and unknown environment. *IEEE Trans. on Industrial Electronics*, 47(2):403–412, April 2000.

[6] R. Koeppe. *Sensorimotor Skill Transfer of Compliant Motion.* PhD thesis, ETH Zürich, 2001. (submitted).

[7] S. Komada, N. Machii, and T. Hori. Control of redundant manipulators considering order of disturbance observer. *IEEE Trans. on Industrial Electronics*, 47(2):413–420, April 2000.

[8] J. De Schutter. Improved force control laws for advanced tracking applications. In *Proc. of the 1988 IEEE Int. Conf. on Robotics and Automation, (ICRA'88)*, pages 1497-1502, USA, 1988.